Semicond. Sci. Technol. **23** (2008) 085024 (10pp) doi:10.1088/0268-1242/23/8/085024

A model of a tunable quantum dot in a semiconducting carbon nanotube

T Kostyrko[1] **and S Krompiewski**[2]

[1] Faculty of Physics, A Mickiewicz University, ul. Umultowska 85, 61-614 Poznań, Poland
[2] Institute of Molecular Physics, Polish Academy of Sciences, ul. M Smoluchowskiego, 17, 60-179 Poznań, Poland

Received 15 May 2008, in final form 18 June 2008
Published 24 July 2008
Online at stacks.iop.org/SST/23/085024

Abstract
We consider a model of a quantum dot (QD) in a semiconducting carbon nanotube, created by using a spatially limited electric potential, produced by a system of a few external elementary charges. Our main interest is in correlated states of a pair of electrons within the dot described in terms of the π-electron Hamiltonian supplemented with electron Coulomb repulsion (the extended Hubbard Hamiltonian). We determine the value of the potential field necessary to keep two extra electrons within the dot and determine the spin symmetry of the two-electron wavefunction. It has been found that the ground state of the two electrons localized in the QD is a triplet for moderate values of the potential and it changes to the singlet state for strong enough potential. Additionally, *ab initio* (SIESTA) computations have been performed for the doubly charged nanotube with a QD due to the presence of two positive ions placed nearby. Remarkably, both the approaches yield consistent results concerning the robustness of the two-electron states within the QD.

(Some figures in this article are in colour only in the electronic version)

1. Introduction

Electronic properties of quantum dots (QDs) with just a few electrons have been intensively studied for quite some time in the context of Coulomb blockade (CB) [1] and Kondo effects [2, 3]. The temperature range of observation of these phenomena in lithographically defined QDs [4], or metallic carbon nanotubes weakly coupled to the leads [5] is usually restricted to a fraction of a Kelvin degree because of a relatively small distance between one-electron energy levels and low values of charging energy. On the other hand, for practical applications, like nanoelectronics, QD working in a room temperature range would be desirable. This can be achieved using smaller, molecular QDs with much higher values of characteristic energy scales. Examples of such systems are for instance a fullerene molecule [6] or a section of a metallic carbon nanotube (CNT) with local barriers (buckles) created by an AFM tip [7] or 5–7 defects [8].

In the present paper we consider a model of a system in which a QD is formed by application of a local electric field [9] near the center of a semiconducting CNT of finite length. Such a field could be created by a properly arranged system of gate electrodes, a set of static external charges, and it can also result from physisorption of molecules with finite dipole moments at the surface of the nanotube. If a field of this type could be controlled in an experiment, one would obtain a local potential well with desirable depth and size, i.e. a tunable QD. In what follows we analyze the electronic structure of the QD for various parameters characterizing the nanotube, interactions between electrons and the strength of the local potential. We determine the minimum value of the potential necessary to keep an electron pair within the dot. In relation to the recent investigations [10, 11] on the stability of triplet states in nanotube quantum dots, we focus on the spin symmetry issue of the lowest energy two-electron states.

In the second part of the paper, we compare the results of the model approach with those obtained using density functional theory (DFT) computations for a nanotube under the influence of a system of external charges. Although the two approaches differ substantially from each other, we find that remarkably, the common feature of both the model approach and the DFT one is the existence of a two-electron state localized at the minimum of the potential well created by the external potential. This allows us to reach conclusions about a possible experimental realization of the tunable QD.

2. The model and approximations

We describe a semiconducting CNT based on a tight-binding Hamiltonian where each carbon atom is represented by a single local π-orbital, and where the total electron band of the neutral CNT is half-filled. This approach allows us to deal adequately with electron states within the distance of a few eV from the Fermi level [12] and properly relate the existence of the electron energy gap to the helicity of the nanotube. The potential created by a system of external charges will be accounted for by the site-energy term, with actual values of the local energy computed each time for the assumed distribution of the external charges. The one-particle Hamiltonian reads

$$\mathcal{H}_0 = t \sum_{\langle \mathbf{PR}\rangle\sigma} c^{\dagger}_{\mathbf{P}\sigma} c_{\mathbf{R}\sigma} + \sum_{\mathbf{R}\sigma} E_{\mathbf{R}} n_{\mathbf{R}\sigma}, \tag{1}$$

where $c^{(\dagger)}_{\mathbf{R}\sigma}$ represents the electron annihilation (creation) operator for carbon at the position indicated by the vector $\mathbf{R}$ and spin σ, $n_{\mathbf{R}\sigma} = c^{\dagger}_{\mathbf{R}\sigma} c_{\mathbf{R}\sigma}$, t is the hopping parameter (assumed here to be our energy unit) and $E_{\mathbf{R}}$ is the site energy for a carbon atom at $\mathbf{R}$.

The long-range Coulomb interactions between extra electrons (with respect to the charge neutrality situation) in the charged CNT are described below as in the extended Hubbard Hamiltonian (or, equivalently, PPP model [13, 14])

$$\mathcal{H}_1 = U \sum_{\mathbf{R}} n_{\mathbf{R}\uparrow} n_{\mathbf{R}\downarrow} + \frac{1}{2} \sum_{\mathbf{P}\neq\mathbf{R}\sigma\sigma'} U(\mathbf{P}-\mathbf{R}) n_{\mathbf{P}\sigma} n_{\mathbf{R}\sigma'}. \tag{2}$$

In equation (2) we single out the on-site (Hubbard) part of the interaction from the long-range part. In what follows we assume for the long-range part a simple $1/R$ dependence, parametrized by the dielectric constant ϵ

$$U(\mathbf{P}-\mathbf{R}) = \frac{1}{\epsilon|\mathbf{P}-\mathbf{R}|}, \qquad \mathbf{P}\neq\mathbf{R}. \tag{3}$$

Such an approach allows us to describe the electron–electron repulsions with the smallest possible number of parameters and to study independently the effects of the local interactions and the long-range ones.

We deal with the above-defined Hamiltonian using a variational approach, which involves the following two steps. We first diagonalize exactly the one-electron Hamiltonian, equation (1), for a given distribution of external charges, and a finite nanotube with open ends. The open-ended CNT exhibits two kinds of solutions: (1) those which extend throughout the whole nanotube, and which correspond either to the valence band or the conduction band states, (2) the end states which appear within the energy gap in the semiconducting nanotube, with their wavefunctions localized near one of the ends of the nanotube [15]. In experiments, the nanotube is usually connected to external leads (contacts), and the end states, if existing, may critically depend on the CNT/contact interfaces. Without going into details about the actual interface problems, we mimic a possible biasing voltage effect by simply applying an extra (asymmetric) potential at the ends of the nanotube.

The main effect of the spatially restricted external potential in a neighborhood of the nanotube is the appearance of the potential well in the nanotube centered near the external charges. The potential well can trap additional electrons or holes depending on the sign of the dominating external charges. At the same time the local energy perturbation may be considered as a defect in the system to which the one-electron structure responds by creation of a localized state (or states) within the energy gap, and centered at the bottom of the potential well. One can then expect that the wavefunctions of the extra electrons in the tube can be, to first approximation, well represented by these localized states. Therefore in the second stage of our approach we construct the wavefunction of the nanotube charged with extra electrons from these localized states. We also include, in our basis, some states from the continuum which are energetically close to the localized states. Specifically, in the case of two extra electrons with z-component of the total spin, $S_z = 0$, we form a two-particle basis as follows:

$$|\lambda\uparrow, \lambda'\downarrow\rangle = a^{\dagger}_{\lambda\uparrow} a^{\dagger}_{\lambda'\downarrow}|0\rangle \tag{4}$$

where λ refers to the one-electron energy level of Hamiltonian (1).

$$a^{\dagger}_{\lambda\sigma} = \sum_{\mathbf{R}} \alpha_{\lambda\mathbf{R}} c^{\dagger}_{\mathbf{R}\sigma} \tag{5}$$

creates an electron in the one-particle state λ and the coefficients $\alpha_{\lambda\mathbf{R}}$ are obtained from the eigenstates of the Hamiltonian (1). The vacuum state in (4) is defined here as the ground state of Hamiltonian (1) corresponding to the neutral nanotube. In what follows we assume that the electron interactions between the extra electrons do not perturb this state. This is the most serious approximation in our approach; it should be justified as long as the energy distance between the lowest in-gap localized state and the top of the valence band is not too small. We can expect that in this case the virtual electron excitations from the valence band to the in-gap states do not modify substantially the interactions between the electrons in the localized states.

In addition to the states with $S_z = 0$, we can also consider states with $S_z = \pm 1$ with the basis:

$$|\lambda\sigma, \lambda'\sigma\rangle = a^{\dagger}_{\lambda\sigma} a^{\dagger}_{\lambda'\sigma}|0\rangle, \qquad (\lambda \neq \lambda'). \tag{6}$$

Using the basis defined by equations (4) and (6) we can now diagonalize the total Hamiltonian, $\mathcal{H} = \mathcal{H}_0 + \mathcal{H}_1$, for the case of two extra electrons in the nanotube, without any further approximations. The matrix elements of the Hamiltonian read, for the $S_z = 0$ case:

$$\begin{aligned}\left\langle \lambda\uparrow, \lambda'\downarrow \right| \mathcal{H} \left| \mu\uparrow, \mu'\downarrow \right\rangle &= U \sum_{\mathbf{R}} \alpha_{\lambda\mathbf{R}}\alpha_{\lambda'\mathbf{R}} \cdot \alpha_{\mu\mathbf{R}}\alpha_{\mu'\mathbf{R}} \\ &+ \sum_{\mathbf{R}\neq\mathbf{R}'} U(\mathbf{R}-\mathbf{R}')\alpha_{\lambda\mathbf{R}}\alpha_{\lambda'\mathbf{R}'} \cdot \alpha_{\mu\mathbf{R}}\alpha_{\mu'\mathbf{R}'} \\ &+ (\varepsilon_\lambda + \varepsilon_\lambda)\delta_{\lambda\mu}\delta_{\lambda'\mu'},\end{aligned} \tag{7}$$

where ε_λ denotes the eigenvalue of Hamiltonian (1). Likewise, for the $S_z = \pm 1$ basis:

$$\begin{aligned}&\langle \lambda\sigma, \lambda'\sigma|\mathcal{H}|\mu\sigma, \mu'\sigma\rangle \\ &= \sum_{\mathbf{R}\neq\mathbf{R}'} U(\mathbf{R}-\mathbf{R}')(\alpha_{\lambda\mathbf{R}}\alpha_{\lambda'\mathbf{R}'} - \alpha_{\lambda\mathbf{R}'}\alpha_{\lambda'\mathbf{R}})\alpha_{\mu\mathbf{R}}\alpha_{\mu'\mathbf{R}'} \\ &+ (\varepsilon_\lambda + \varepsilon_\lambda)\,\delta_{\lambda\mu}\delta_{\lambda'\mu'}, \qquad (\lambda \neq \lambda', \mu \neq \mu').\end{aligned} \tag{8}$$

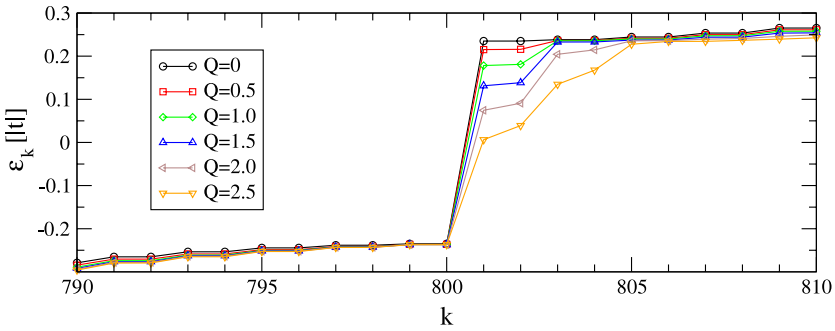

Figure 1. Single particle energy eigenvalues near ε_F for (8, 0) CNT (50 u.c.), for several values of the dipole field. The eigenvalues are labelled with a mode index k in ascending order, and ε_{800} corresponds to the highest occupied single particle level in the case of the neutral CNT. The strength of the dipole field is determined by the dimensionless value Q (see the text). We used here, and in all other figures in this section, the antisymmetric potential at the ends to eliminate the end states from the vicinity of ε_F.

Note that the matrix elements for the triplet states do not depend on the local repulsion. The two-particle eigenstates of interacting electrons can be represented by linear combinations of the basis states, equations (4) and (6),

$$|\Psi^{(0)}\rangle = \sum_{\lambda\lambda'} \gamma_{\lambda\lambda'} |\lambda\uparrow, \lambda'\downarrow\rangle,$$
$$|\Psi^{(2\sigma)}\rangle = \sum_{\lambda\lambda'} \gamma_{\lambda\lambda'} |\lambda\sigma, \lambda'\sigma\rangle, \tag{9}$$

with the coefficients $\gamma_{\lambda\lambda'}$ being eigenvectors of the matrix (7) or (8).

3. Results of the model approach

In this section we present the numerical results of the variational approach for the model Hamiltonian. We perform most of our computations on zigzag nanotube (8, 0) of finite length. This nanotube is wide enough so that the σ–π rehybridization effects are negligible near the Fermi level and the nanotube is semiconducting both within the tight-binding method and according to the *ab initio* calculations [16, 17]. The problem of two interacting electrons is solved within the basis of states defined by equations (4) and (6). The convergence of the computations has been controlled by comparing the results obtained for bases of different sizes. In the region of the parameters we used here, the basis including altogether 14 states (all the in-gap localized states plus several of the extended ones from the conduction band) has been found to be sufficient to obtain the desired accuracy. The quality of our approximation relies on the existence of the energy separation between the in-gap localized states and the continua of both the valence and conduction bands. In consequence this approach should be valid for the nanotubes of an arbitrary chirality, provided they are semiconducting.

Figure 1 shows a single-particle energy spectrum near the Fermi energy ε_F for (8, 0) CNT of 50 unit cells (u.c.), for several values of electrostatic dipole potential. The dipole field creates a potential well for electrons at the middle of the CNT. In this section we consider a dipole consisting of two charges: $+Q|e|$, $-Q|e|$ separated by 3 Å from each other and placed at the same distance from the nanotube surface. The dipole moment is directed transversely to the nanotube axis.

As is well known from many previous studies of the carbon nanotubes [18–20], due to one-dimensional structure of these systems an arbitrary small local potential leads to the appearance of a localized state near the bottom or the top of the band, depending on the sign of the potential. In conducting CNTs no localized states exist near ε_F, since they would have been degenerate with the extended states. Instead, the resonance states are formed. In the present case of the semiconducting CNT the true localized states can exist near ε_F, due to the vanishing density of states below the bottom of the conduction band. As can be seen in figure 1 the application of the local potential leads to the appearance of a number of states in the gap region, and the number grows with the strength of the potential. All the in-gap states differ from the states of the valence band and the conduction band in that their energy clearly depends on the potential strength. This shows that they are concentrated near the bottom of the potential well and thus localized.

A special feature of the CNTs directly related to the symmetry of their structure is a double degeneracy of the single particle levels. This feature could be observed in the localized states as well, if the external potential had the same symmetry as that of the CNT. Otherwise, for realistic external potentials one can expect some perturbation of the rotational symmetry. Indeed for our choice of the potential one can see in figure 1 that the tendency for the degeneracy, seen for a small value of the potential, is gradually destroyed by the increase of the potential strength. As we show below this appears to have an important effect for the spin symmetry of the two-electron localized ground state.

For a definite confirmation of the localized character of the in-gap states we need to analyze the spatial dependence of the corresponding wavefunctions. The single-particle eigenstates of the model (1) can be represented in terms of linear combinations of the local π orbitals, that define $\mathcal{H}_0$. In figure 2, envelopes of the wavefunctions of the six lowest unoccupied single particle states for the neutral CNT ((8, 0), 50 u.c.) are shown, for the dipole with charges $\pm e$ (i.e. $Q = 1$). The value of the envelope for each unit cell has been computed here as a maximum of the squared coefficients used in the expansion of the wavefunction in local orbitals. One can see from the figure that for the given value of the local potential

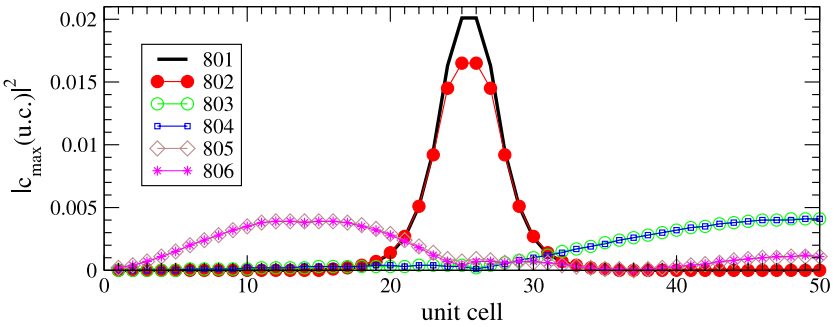

Figure 2. The envelopes of the wavefunctions of the six lowest unoccupied single particle states (for CNT (8, 0), 50 u.c.), for the dipole charges $\pm e$ ($Q = 1$).

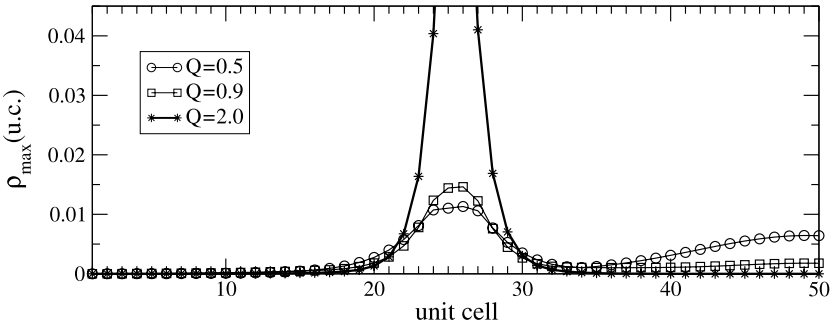

Figure 3. The envelope of the electron density related to the lowest two-particle states of the CNT ((8, 0), 50 u.c.) charged with two extra electrons, for several values of the dipole field, $U = 1$ and $\epsilon = 2.0$. For $Q = 0.5$ the envelope shows a two-particle ground state with one of the electrons in the potential well and the other in the extended state, whereas the envelope for $Q = 2$ is typical for the two-electron state with both electrons localized in the well.

only the first two, of the shown six lowest unoccupied energy levels, are localized. This is in agreement with the result plotted in figure 1, which shows that for $Q = 1$ only two energy levels (namely 801 and 802) are clearly split from the conduction band.

The electronic structure of the double charged CNT is in our model reduced to the problem of two interacting particles in the external local potential. The direct analysis of the two-electron wavefunction would be complicated in this case because of the absence of translational invariance. Instead, we study the spatial dependence of the electron density in the two-particle ground state. The electron density along the nanotube can be computed from the two-particle eigenstates of the matrix (7) as

$$\rho_{\mathbf{R}} = \sum_{\sigma} \langle \Psi^{(S_z)} | n_{\mathbf{R}\sigma} | \Psi^{(S_z)} \rangle. \tag{10}$$

In figure 3 the electron density is shown using the envelope of the density for three representative ground states, for $U = 1$ and $\epsilon = 2$. For $Q = 0.5$ the depth of the potential well is too small to accommodate two electrons in the well, because of the repulsion between the electrons, and the ground state of the system is obtained for one electron localized in the well with the other in the extended state. In this case the increase in energy resulting from the mutual electron repulsion is very small in view of large spatial separations of electrons. Incidentally, it is interesting to note in this context that the above-mentioned scenario resembles the case of 'a small dot within a large dot' [21], in a conventional heterostructure, where new functionalities have been predicted (singlet–triplet filtering and entanglement).

With increase of the dipole potential the tendency for both the electrons to become localized in the well increases, as can be seen from the decrease of the contribution from the extended state for $Q = 0.9$. For $Q = 2.0$, both the electrons are localized in the well and the contribution from the extended state is negligible.

The evolution of the spatial extension of the two-particle localized ground state is clearly seen in the semi-logarithmic plot of the envelopes of the electron density (figure 4). As expected, the slope steepness of the electron density gradually grows with increasing depth of the potential well.

In this paper we study the two-particle solutions for the model of CNT of finite length. This does not allow us to formulate a strict criterion of localization of the various solutions, which can only be found in the limit of infinitely long nanotubes. Instead, we use an approximate formal criterion for localization of two electrons in the potential well in the ground state. For this purpose we define a quantity

$$\Delta_{\mathrm{loc}} = \varepsilon_{\mathrm{loc}} + \varepsilon^{(0)}_{LUMO} - \mathcal{E}_0. \tag{11}$$

Here, $\varepsilon_{\mathrm{loc}}$ is the smallest energy of unoccupied one-particle localized states which is split from the conduction band by the external local potential, $\varepsilon^{(0)}_{LUMO}$ denotes the lowest unoccupied single particle state in the absence of the external potential and $\mathcal{E}_0$ is the ground-state energy of the two-particle state (i.e. eigenvalue of the matrix (7)). The value of $\varepsilon^{(0)}_{LUMO}$ is a good measure of the smallest energy of the extended state in the

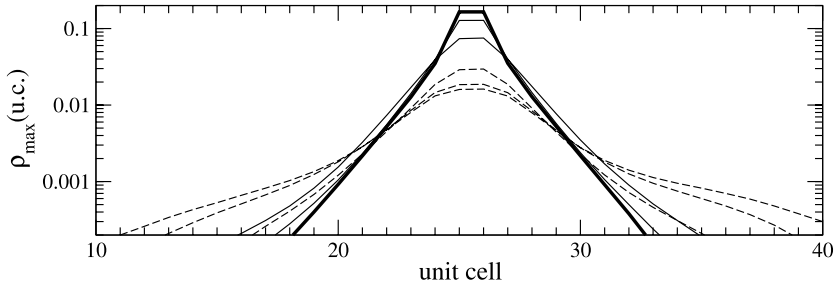

Figure 4. The semi-logarithmic plot of envelopes of the electron density of the fully localized two-electron states of the CNT ((8, 0), 50 u.c., $U = 1$, $\epsilon = 2$) with two extra electrons, for several values of the dipole field ($Q = 1.0, 1.1, 1.5, 1.8, 2.5, 3.0$: the maximum of the envelopes increases with Q).

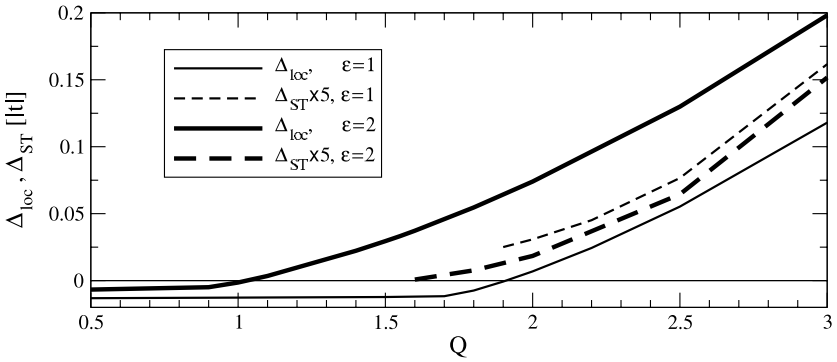

Figure 5. Values of $\Delta_{\rm loc}$ and Δ_{ST} providing criteria of stability of different two-particle ground states (see the text) as a function of the local potential strength for two values of the dielectric constant. The dashed curves cover the stability range of the two-electron localized states.

conduction band (see figure 1). We can, to a fairly good approximation, neglect the interactions between electrons if one of them occupies the extended state of the conduction band while the other is localized in the well, since they are rather well spatially separated from each other (see figure 2). Therefore, the value $\Delta_{\rm loc}$ allows us to compare the energy of the fully localized two-electron state with that when only one of the electrons remains in the potential well and the other is in the extended state. The solution of the equation $\Delta_{\rm loc} = 0$ separates areas of existence of the fully localized two-electron states from the other states in the parameter space of our model.

We also compare the energy of the lowest two-particle solution for $S_z = 0$ with the corresponding solution for $S_z = \pm 1$ eigenspace, and define in this way a singlet–triplet energy difference, $\Delta_{ST} = \mathcal{E}_0^{(\pm 1)} - \mathcal{E}_0^{(0)}$. A stability region of the singlet solutions is defined by $\Delta_{ST} > 0$, whereas $\Delta_{ST} = 0$ means that the triplet state is the stable one. Note that because of the spin rotational invariance of our model, each of the eigenstates from the $S_z = \pm 1$ subspace has its counterpart of the same energy in the $S_z = 0$ subspace. In figure 5 we plot the values of $\Delta_{\rm loc}$ and Δ_{ST} as functions of the local potential strength for two values of the dielectric constant. The value of $\Delta_{\rm loc}$ provides an energy scale determining the stability of the two-electron localized state and it is typically a fraction of the hopping parameter. The value of the singlet–triplet energy difference is usually much smaller than $\Delta_{\rm loc}$ (note that in figure 5 it is multiplied by 5 and it slowly decreases with increasing ϵ).

The stability diagram obtained in this way is presented in figure 6. The diagram is not universal and it depends on details of the spatial dependence of the external potential and the model of long-range repulsion. It can however be useful for a qualitative discussion of stability conditions of the solutions. In general, the bigger the local potential the more stable the fully localized two-particle state, analogously to the behavior of single particle energy levels presented in figure 1. Increase in the stability of the fully localized two-particle state with the dielectric constant can be understood as the asymptotic case ($\epsilon \to \infty$), where only the local (on-site Hubbard) electron repulsion is important. The existence of two nearly degenerate localized single particle levels for a small but finite local potential stabilizes the triplet solution ($S_z = \pm 1, 0$) with two electrons in the different single particle energy levels. Since the local repulsion does not contribute to the energy of the triplet state at all (cf equation (8)), the two-particle fully localized state in the $\epsilon \to \infty$ limit will be stable for an arbitrarily small finite local potential. For finite ϵ one needs to apply a sufficiently strong local potential to overcome the effect of the long-range repulsion and stabilize a fully localized two-particle state. With further increase in the potential that breaks the rotational symmetry of the CNT and removes the degeneracy of the localized single particle levels, it may be more favorable for the electrons to occupy the same lowest energy level at the cost of increase of the contribution from the Hubbard repulsion. Therefore for the strong enough local potential the singlet solution becomes more stable, provided that the U is not too strong. The effect

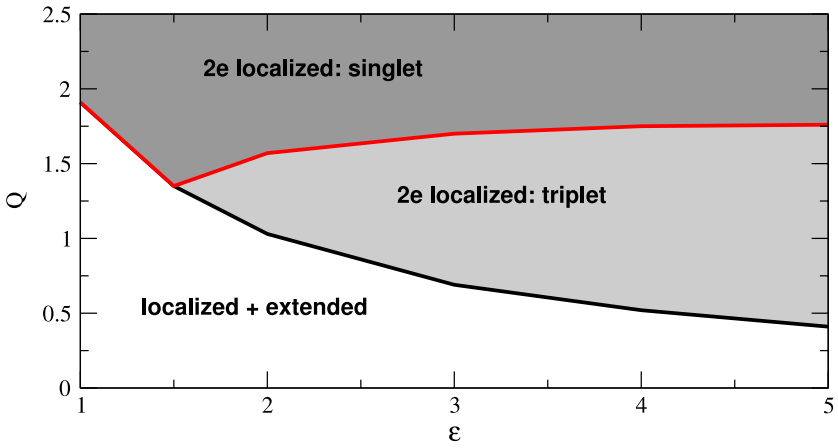

Figure 6. The stability diagram of different two-particle ground states for CNT ((8, 0), 50 u.c.) charged with two extra electrons for $U = 1$.

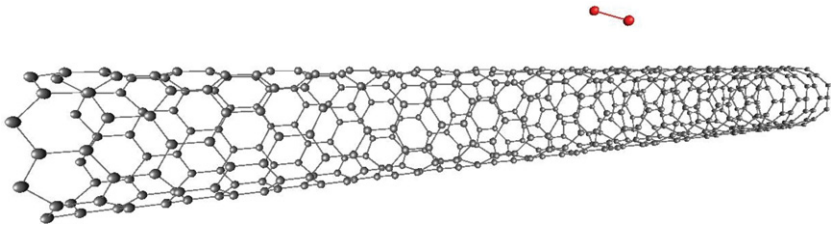

Figure 7. CNT (8, 0), 30 u.c., and a system of two static charges.

of long range interactions on the singlet and triplet states is similar. Therefore the energy difference between the singlet and triplet solutions, Δ_{ST}, will depend mainly on the energy balance between the splitting of two lowest localized single particle levels and the average value of the local repulsion in the singlet ground state. The former value would depend on the spatial extension of the localized single particle state determined by both the strength of the local potential and the distribution of external charges.

4. Results of the DFT computations

The model approach we discussed so far has some obvious limitations, such as a restricted atomic basis or lack of selfconsistency in the computation of the one-particle electronic structure. In order to check if the main conclusions obtained in the model computations remain true in a more advanced approach, we use a density functional theory (DFT) in a version implemented in the SIESTA package [22].

SIESTA is based on the pseudopotential method, which significantly reduces the number of electronic degrees of freedom and is quite sufficient if one deals with an electronic structure not too far from the Fermi level. The package uses linear combination of atomic orbitals (LCAO) basis with pseudoatomic orbitals (PAO) of finite range in a solution of the Kohn–Sham (KS) equations. The aforementioned features of SIESTA make it applicable for studies of the relatively large system ($\sim 10^3$ C atoms) we deal with.

We study a system composed of a fragment of CNT (8, 0), specifically 15 and 30 CNT unit cells. As a source of the external potential we take two alkali atoms, separated from the CNT surface by 4 Å (see figure 7). This time, we eliminate the end states from the electronic structure, by application of the periodic boundary conditions, along the CNT axis. Since our unit cell of the compound system includes up to 960 C atoms, we are forced to use the simplest (SZ, i.e. single-zeta) basis to describe the C atoms. In this basis each valence orbital is described by a single PAO. Although this basis is good basically for qualitative analysis it can correctly predict metallic or semiconducting properties of CNTs. For the two alkali atoms we restricted our basis to s orbitals with a very small radius in order to move all the energy eigenvalues of the alkali atoms much above the Fermi level of the CNT and, at the same time, to avoid any overlap between alkali atom- and CNT-wavefunctions. In effect the s-electrons of the alkali atoms have been completely transferred to the CNT. We thus end up with double charged ($-2|e|$) CNT and a system of two positive charges centered at the positions of the alkali atoms. In the self-consistent DFT scheme, used in the solution of the KS equations, all the electrons could then feel selfconsistent dipole potential of the order of 50 D. As a result, we could expect at least some qualitative agreement between the previously described model calculations and the present DFT ones.

All the numerical results presented below are obtained using the Troullier–Martins pseudopotential [23] and the local density approximation (LDA) [24] for the exchange-correlation potential. To determine the PAO radius for C atoms we set the PAO energy shift [22] to 0.02 Ry. In figure 8 we show KS energy values for the system described in figure 7, where the eigenvalues are indexed in ascending order, as in

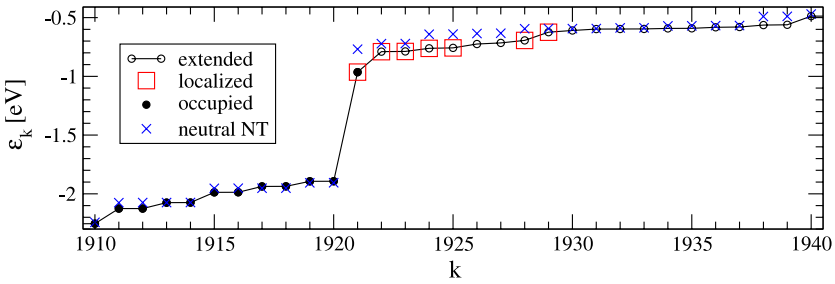

Figure 8. The single particle Kohn–Sham (KS) energy values for a CNT ((8, 0), 30 u.c. with the periodic boundary conditions) charged with two electrons, under the influence of a potential created with two static charges of value $+|e|$ each, positioned as in figure 7. The energy values are labelled with the mode index k in ascending order (see figure 1 to compare with the results of the model calculations). In the figure the KS eigenvalues (uniformly shifted for comparison) for the neutral CNT in the absence of the external potential are also shown with crosses.

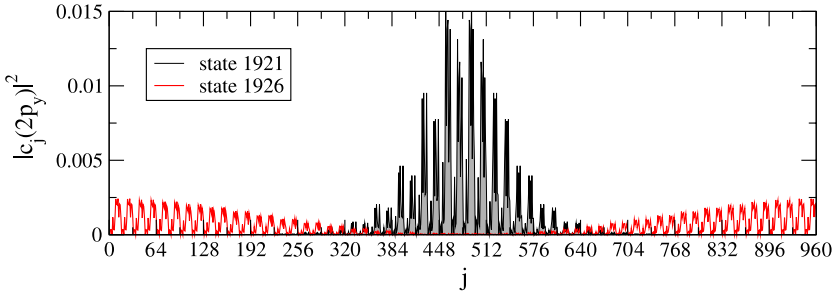

Figure 9. The squared coefficients of the expansion of the KS eigenstate in the atomic orbitals versus atom index for the HOMO level (state 1921, shaded area), and for the lowest extended orbital (state 1926), for the CNT as in figures 7 and 8. Here, only dominating $2p_y$ components are shown.

figure 1 corresponding to the model calculations. In the absence of any local potential, the CNT (8, 0) has a fairly large energy gap of the order of 1 eV (incidentally, in our calculation the gap is somewhat overestimated, mainly due to the small basis set we use) and the Fermi level is positioned near the middle of the gap. Application of the local potential deforms first the conduction band close to ϵ_F, whereas the shape of the valence band near ε_F is hardly changed. The conduction band is most deformed near its bottom and one can see an isolated state (1921) which is split by about 0.2 eV from this band. From the computed position of the Fermi level, $\varepsilon_F = -0.89$ eV, as well as from the state counting argument and the balance of the charge in the system, we conclude that this state is the HOMO state in the present case.

In figure 9 the HOMO state is plotted together with the lowest unoccupied extended state, and we confirm the expectation that it is very well localized near the position of the two external charges as in the model calculations. Note also that the lowest extended state is well separated from the localized one, very much like in figure 2.

In order to see how the extra charge is distributed along the CNT, we plot the results of the Mulliken population analysis from the SIESTA calculation (figure 10). Comparison with the spatial dependence of the localized HOMO state shows that the distribution of the charge can be fairly well explained by assuming that all the extra charge goes to the new HOMO state and the rest of the occupied states does not change much as compared to the case of the neutral CNT. This seems in agreement with the previous observation concerning relatively high rigidity of the valence band, seen in figure 8.

In figure 11 we present a plot of the envelope of the KS localized states, indicated in figure 8. Since the KS states provide the density of the interacting system in the DFT computations, this can be qualitatively compared with the plots of the electron density obtained from the model computations (figure 4). It is noteworthy that the HOMO state is indeed very well localized (as can be concluded on the basis of almost linear dependence of the envelope function with the distance from the center of the local potential in this semi-log plot). Moreover it can readily be seen that the localization radius increases (although not quite monotonically) with the increase in energy of the state.

On the one hand, the DFT (SIESTA) computations confirm the most important result of the model approach which is the existence of a stable localized two-electron state induced by the external potential. On the other hand, however, SIESTA predicts that a stable solution is the singlet one. From our computations performed for CNT (8, 0), of both 15 u.c. and 30 u.c. in length, the stable solution with the total spin $S_z = +1$ has been found to be higher in energy by about 0.1 eV than the $S_z = 0$ state. The latter result cannot however be regarded as decisive since it may get modified for other exchange-correlation potentials, more appropriate for strong correlations.

5. Summary and conclusions

In this paper we have demonstrated a possibility of creating and controlling a quantum dot in a semiconducting carbon

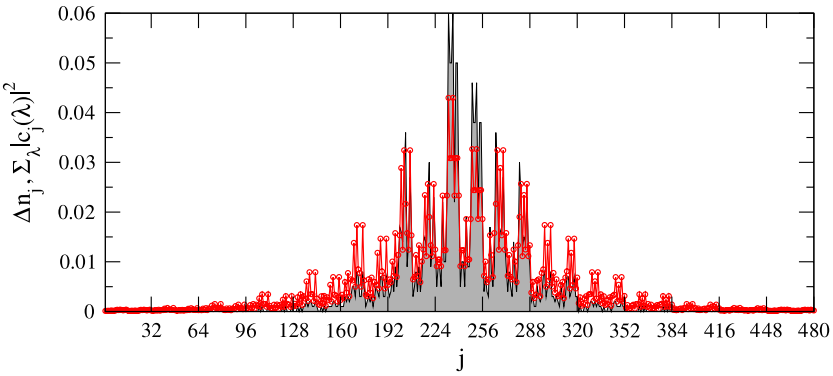

Figure 10. The excess Mulliken populations, i.e. $\Delta n(j) = n_{2e}(j) - n_0(j)$, where $n_{0(2e)}$ denotes the population for the neutral (charged) nanotube, along the CNT (as in figures 7 and 8, but for 15 unit cells; gray shaded area), compared with the sum of squared coefficients of all the valence orbitals ($\lambda = 2s, 2p_x, 2p_y, 2p_z$), for the doubly occupied, localized HOMO level (open circles). For the sake of comparison, the sum of the coefficients of the wavefunction was multiplied by 2 to account for the double occupancy of this level.

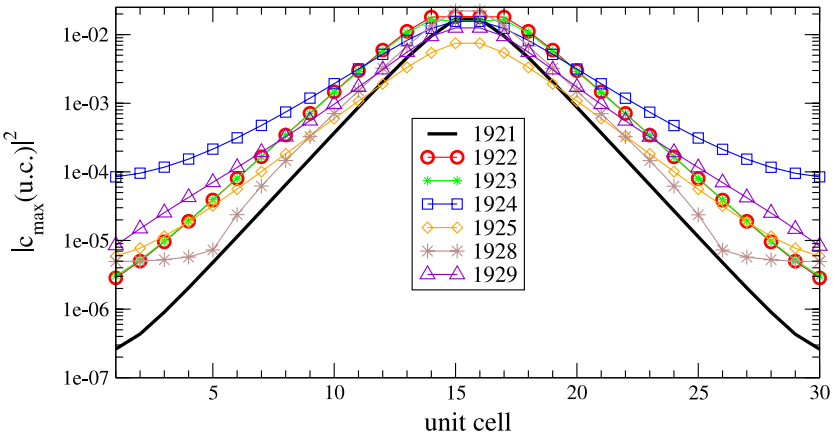

Figure 11. The semi-logarithmic plot of the envelopes of squared coefficients of dominating components of all the KS localized states shown in figure 8 (this can be compared with figure 4 obtained from the model computations).

nanotube with the help of electrostatic potential induced by a system of a few external charges. It should be stressed that what we mean by the dot is a segment of the CNT defined by the potential well. This is to be contrasted with a more common definition of the CNT dot—meant as an entire nanotube, usually a metallic one, confined by external contacts—that most experimental and theoretical works deal with [30–33]. Consequently, the new physics (and related potential applications) that comes about in the present case is due to substantial enhancement of correlations, resulting in increasing of charging energy and stabilizing the triplet multiplicity up to energies corresponding to room temperature. The latter case might open opportunities for controlling the spin both magnetically (external magnetic field) and electrically (external potential and/or gate voltage) in future spintronic devices.

We analyzed the stability of different solutions for the case of two extra electrons in the semiconducting CNT, using the model Hamiltonian and the SIESTA DFT method. We have found that both the model approach and the DFT-based one predict a stable solution with two electrons localized in the well created by the potential. As concerns the qualitative features of the dependence of the one-electron spectrum on the strength of the local potential, as well as the density distribution for the electrons localized in the dot, these two approaches agree quite well.

Within the model approach we have found the threshold value of the local potential necessary to keep both extra electrons in the dot. This value decreases with increase in the dielectric constant in the long range repulsion between electrons. For moderate values of the local potential above the threshold, the lowest energy solution corresponds to the triplet state. The singlet state becomes stable only for a strong enough potential.

The stability of the triplet state is related to the well-known double degeneracy of orbital states related to the possibility of clockwise and anticlockwise motion of electrons around the tube. In experiments with the whole CNT treated as the QD, this degeneracy can be lifted by application of the magnetic field parallel to the axis of the CNT [10], which allows one to observe the triplet to singlet transitions with increase of the strength of the field. In the case studied here, in the presence of the local potential the extra electrons are confined to the relatively small region of the potential well. Therefore the energetic gain for the electrons which remain in the triplet state as compared to the singlet one is considerably higher than in the case of the whole nanotube treated as the QD, because in the latter case the effective values of electron interactions

may be orders of magnitude smaller. As a result the triplet state is stable for moderate values of the local potential, when the energy difference of the lowest in-gap single-particle localized levels is still relatively small. With increase in the strength of the potential this degeneracy is completely lifted and consequently the singlet solution gets stabilized.

The SIESTA DFT results predict that the singlet solution is more stable than the triplet one. This might seem inconsistent with the predominantly triplet ground state in the model computations, especially for larger values of U. Unfortunately within the SIESTA package we have rather limited control over relevant parameters. In particular, it is impossible to match them in a precise way with the tight-binding model parameters. For this reason we cannot definitively say whether there is an actual discrepancy in the two approaches or just that the DFT results correspond to the singlet state stability region in the model approach. Moreover the DFT–LDA conclusion about the relative stability of the singlet solution over the triplet one should be treated with caution, since it is well known that standard exchange-correlation potentials need usually serious modifications (self-interaction or generalized gradient corrections, L(S)DA+U, etc) when applied to strongly correlated systems.

Besides, no one-to-one relationship between the DFT results and the model-based ones can be expected because of the simplifications involved in the model formulation, such as restriction of the hopping integrals to the nearest neighbors only and neglect of σ-orbitals. Moreover, the neutral reference state of the carbon nanotube has been computed in the non-selfconsistent way in the model approach. All these limitations may influence a subtle competition between the singlet and triplet configurations. Another important issue relevant for the comparison with the experiment, is related to the spin–orbit (SO) interaction. Despite the fact that SO coupling is relatively small in elemental carbon (small atomic number), in the case of carbon nanotubes it leads to an important effect consisting in removing the aforementioned double degeneracy of orbital levels, as recently reported [35]. In principle one could extend the present theory along the line developed by Ando [36] and Huertas-Hernando *et al* [37], to incorporate the SO coupling into the tight binding model of interacting electrons in the presence of the local potential. However in the present case the degeneracy of the orbital levels is already removed by the application of the local potential. A comparison of the values of singlet–triplet splitting obtained here, which are typically of the order of $10^{-2}|t| \sim 200$ K (for $|t| \sim 2.5$ eV), with the value of the observed SO coupling being of the order of 2 K, suggests that SO coupling is too small to modify the general features of the stability diagram presented in figure 6 as far as the double occupied QD is concerned. Nevertheless, the SO effects may be important near the boundaries between the stability regions of the different solutions, and in the region where one of the electrons occupies the well and the other is in the extended state. Most probably in these boundary regions the QD ground state is neither purely singlet nor triplet in nature any longer but entangled (see [35]). Otherwise it is important to realize that in the present studies, the spatial confinement of the extra electrons to the small region of the potential well implies that relevant energy scales are rather large. In particular, this applies to the relatively big singlet–triplet splitting, resulting from the enhanced role of the Coulomb interactions.

In fact it is well known that in many carbon-based nanostructures, magnetic moments can be acquired. Typically, it is the case when there are undercoordinated C atoms (with unsaturated bonds) located for instance either close to structural defects [25] or in the vicinity of sample edges [26, 27]. Moreover, itinerant ferromagnetism has been predicted theoretically in heterostructured C/BN nanotubes [28]. Our results show that uncompensated spins can also appear in electron-correlated quantum dots in CNTs. As already mentioned before, the local external electric potential used to create the QD influences the local band structure in a way similar to any other disturbance (including vacancies), so there is no surprise that it can also lead to formation of unsaturated spins. This finding seems to be relevant for prospective spintronic applications due to the relative ease of fabrication and good tunability of the CNT QDs.

Finally some comments are due concerning the possible realizations of the tunable QD in semiconducting CNTs. The main difficulty to overcome consists in finding a spatially limited and at the same time sufficiently strong source of a controllable electrostatic potential, which may not be an easy task. The most obvious candidates seem an AFM tip, or a system of metallic tubes crossing over a semiconducting tube technique [34], or an extra axial-symmetric ring surrounding the semiconducting CNT [29]. One could also use naturally present or artificially created defects gated with the help of a charged AFM tip as was done in metallic nanotubes [38, 39] to obtain a spatially limited and partially tunable device similar to that proposed here. Although the quantum well states of our main interest lie deep in the energy gap, they can participate in electrical transport, possibly via a mechanism analogous to charge pumping driven by surface acoustic waves [40].

Acknowledgments

This work, as part of the European Science Foundation EUROCORES Programme SPINTRA, was supported by funds from the Ministry of Science and Higher Education as a research project in years 2006–2009 and the EC Sixth Framework Programme, under contract no. ERAS-CT-2003-980409. This work is also supported by the Ministry of Science and Higher Education (Poland), the project RTNNANO contract no. MRTN-CT-2003-504574, as well as the EU grant CARDEQ contract no. IST-021285-2. Parts of our numerical work were done with the computer facilities of Solid State Theory Division of TAM.

References

[1] Kouwenhoven L P, Austing D G and Tarucha S 2001 *Rep. Prog. Phys.* **64** 701
[2] Nygård J, Cobden D H and Lindelof P E 2000 *Nature (London)* **408** 342
[3] Hanson R, Kouwenhoven L P, Petta J R and Tarucha S 2007 *Rev. Mod. Phys.* **79** 1217

[4] Goldhaber-Gordon D, Shtrikman H, Mahalu D, Abusch-Magder D, Meirav U and Kastner M A 1998 *Nature* **391** 156
[5] Bockrath M, Cobden D H, McEuen P L, Chopra N G, Zettl A, Thess A and Smalley R E 1997 *Science* **275** 1922
[6] Porath D, Levi Y, Tarabiah M and Millo O 1997 *Phys. Rev.* B **56** 9829
[7] Postma H W Ch, Teepen T, Yao Z, Grifoni M and Dekker C 2001 *Science* **293** 76
[8] Chico L, López Sancho M P and Muñoz M C 1998 *Phys. Rev. Lett.* **81** 1278
[9] Kinder J M and Mele E J 2007 *Preprint* arXiv:0711.0949
[10] Jarillo-Herrero P, Kong J, van der Zant H S J, Dekker C, Kouwenhoven L P and De Franceschi S 2005 *Phys. Rev. Lett.* **94** 156802
[11] Makarovski A, An L, Liu J and Finkelstein G 2006 *Phys. Rev.* B **74** 155431
[12] Mayer A 2004 *Carbon* **42** 2057
[13] Pariser R and Parr R G 1953 *J. Chem. Phys.* **21** 466
Pople J A 1953 *Trans. Faraday Soc.* **49** 1375
[14] Zhao H and Mazumdar S 2004 *Phys. Rev. Lett.* **93** 157402
[15] Rubio A, Sánchez-Portal D, Artacho E, Ordejón P and Soler J M 1999 *Phys. Rev. Lett.* **82** 3520
[16] Blase X, Benedict L X, Shirley E L and Louie S G 1994 *Phys. Rev. Lett.* **72** 1878
[17] Gülseren O, Yildirim T and Ciraci S 2002 *Phys. Rev.* B **65** 153405
[18] Kostyrko T, Bartkowiak M and Mahan G D 1999 *Phys. Rev.* B **59** 3241
[19] Choi H J, Ihm J, Louie S G and Cohen M L 2000 *Phys. Rev. Lett.* **84** 2917
[20] Chico L and Jaskólski W 2004 *Phys. Rev.* B **69** 085406
[21] Giavaras G, Jefferson J H, Fearn M and Lambert C J 2007 *Phys. Rev.* B **75** 085302
[22] Ordejón P, Artacho E and Soler J M 1996 *Phys. Rev.* B **53** R10441
Soler J M, Artacho E, Gale J D, García A, Junquera J, Ordejón P and Sánchez-Portal D 2002 *J. Phys.: Condens. Matter* **14** 2745
[23] Troullier N and Martins J L 1991 *Phys. Rev.* B **43** 1993
[24] Perdew J P and Zunger A 1981 *Phys. Rev.* B **23** 5048
[25] Kim Y H, Choi J, Chang K J and Tomanek D 2003 *Phys. Rev.* B **68** 125420
[26] Okada S and Oshiyama A 2003 *J. Phys. Soc. Japan* **72** 1510
[27] Son Y W, Cohen M L and Louie S G 2006 *Nature* **444** 347
[28] Choi J, Kim Y H, Chang K J and Tomanek D 2003 *Phys. Rev.* B **67** 125421
[29] Barraza-Lopez S, Rotkin S V, Li Y and Hess K 2005 *Europhys. Lett.* **69** 1003
[30] Liang W, Bockrath M and Park H 2002 *Phys. Rev. Lett.* **88** 126801
[31] Moriyama S, Fuse T, Suzuki M, Aoyagi Y and Ishibashi K 2005 *Phys. Rev. Lett.* **94** 186806
[32] Sapmaz S, Jarillo-Herrero P, Kong J, Dekker C, Kouwenhoven L P and van der Zant H S J 2005 *Phys. Rev.* B **71** 153402
[33] Mayrhofer L and Grifoni M 2007 *Preprint* arXiv:0708.1486
[34] McEuen P L 2000 *Phys. World* **13** (June) 31
[35] Kuemmeth F, Ilani S, Ralph D C and McEuen P L 2008 *Nature* **452** 448
[36] Ando T 2000 *J. Phys. Soc. Japan* **69** 1757
[37] Huertas-Hernando D, Guinea F and Brataas A 2006 *Phys. Rev.* B **74** 155426
[38] Woodside M T and McEuen P L 2002 *Science* **296** 1098
[39] Park J Y 2007 *Appl. Phys. Lett.* **90** 023112
[40] Leek P J, Buitelaar M R, Talyanskii V I, Smith C G, Anderson D, Jones G A C, Wei J and Cobden D H 2005 *Phys. Rev. Lett.* **95** 256802